Large-scale hydrodynamic instabilities and structures in protoplanetary disks

Min-Kai Lin
mklin924@cita.utoronto.ca

Canadian Institute for Theoretical Astrophysics

January 31 2014

Research interests

- Astrophysical fluid dynamics of accretion/protoplanetary disks
- Disk-planet interactions, orbital migration
- Self-gravitating disks
- Disk instabilities
- Magneto-hydrodynamics (new)
- Non-linear numerical simulations (FARGO, ZEUS, PLUTO)
- Linear hydrodynamics

Today: large-scale structures in astrophysical disks

Sub-structures in protoplanetary disks

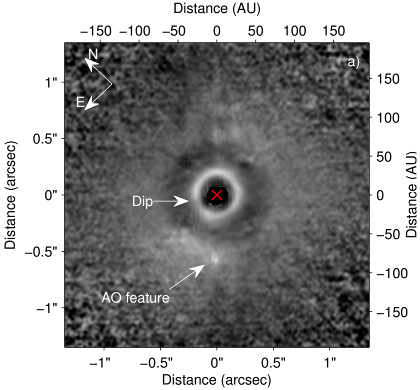

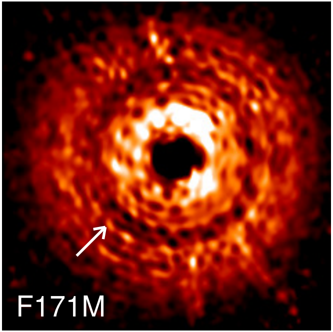

(TW Hya, Debes et al., 2013)

(HD 169142, Quanz et al., 2013)

Non-axisymmetric structures

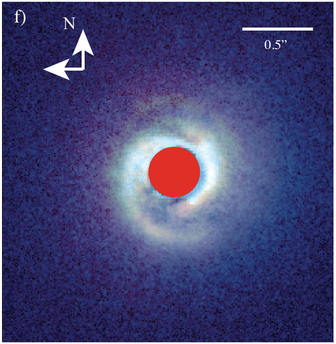

(MWC 758, Grady et al., 2013)

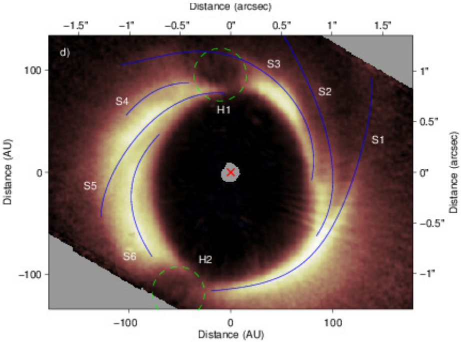

(HD 142527, Avenhaus et al., 2014)

Non-axisymmetric structures

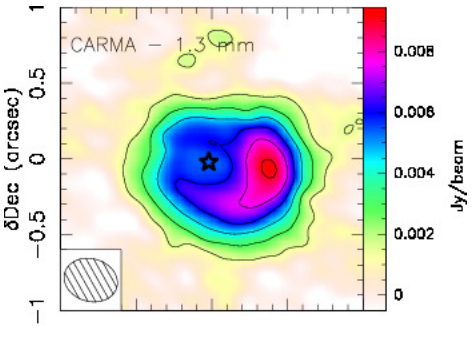

(LkHa 330, Isella et al., 2013)

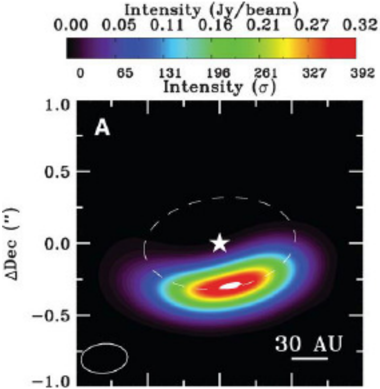

(Oph IRS 48, van der Marel et al., 2013)

Theoretical motivations

- Angular momentum transport: by vortices and non-local transport by waves (Li et al., 2001; Lyra & Mac Low, 2012)
- Dust concentration by vortices $\rightarrow$ planetesimal formation (Barge & Sommeria, 1995; Lyra & Lin, 2013)
- Modifying planet migration (Lin & Papaloizou, 2010)
- Non-axisymmetric instabilities $\leftrightarrow$ underlying disk structure
  e.g. planet gaps and 'dead zones' $\rightarrow$ localized radial gradients

Theoretical motivations

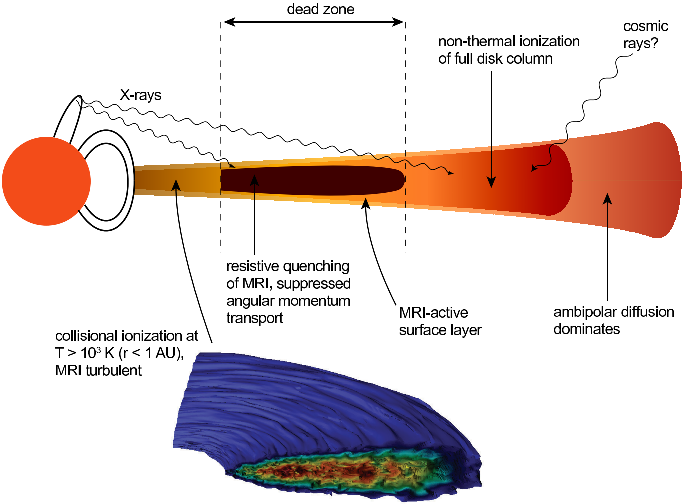

(Armitage, 2011)

Toy model: axisymmetric over-dense ring

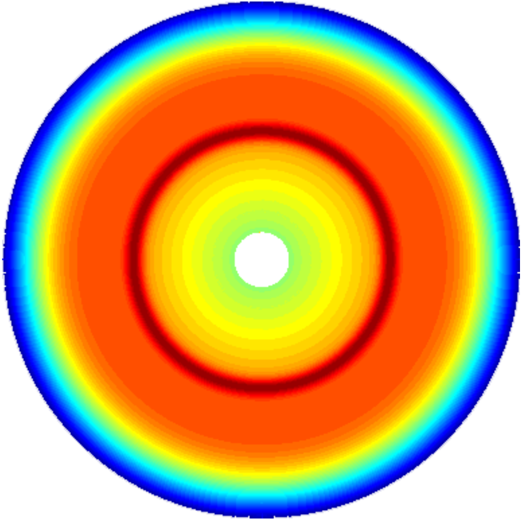

Rossby wave instability

- Kelvin-Helmholtz instability in a rotating disk (Lovelace et al., 1999)
- Thin-disk version of the Papaloizou-Pringle instability (Papaloizou & Pringle, 1985)

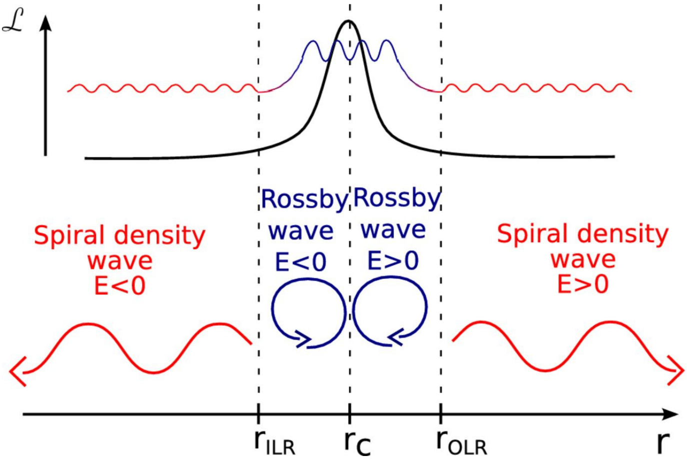

(Meheut et al., 2013)

Vortex formation via the RWI

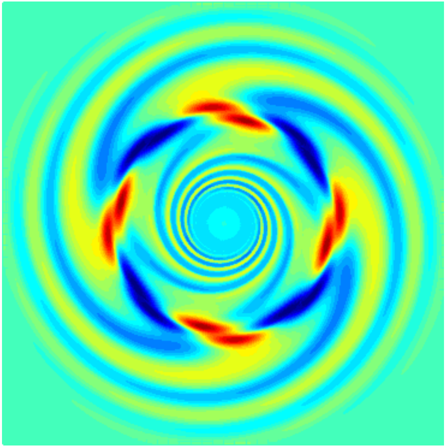

ATHENA code: 3D disk in a box

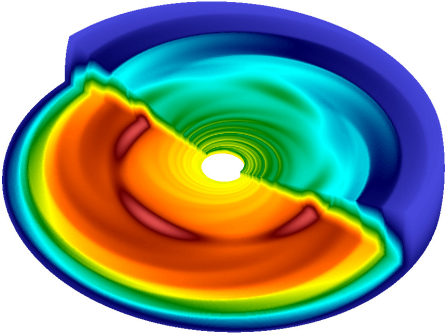

ZEUS code: 3D self-gravitating adiabatic disk, spherical grid

Vortex formation via the RWI

PLUTO code

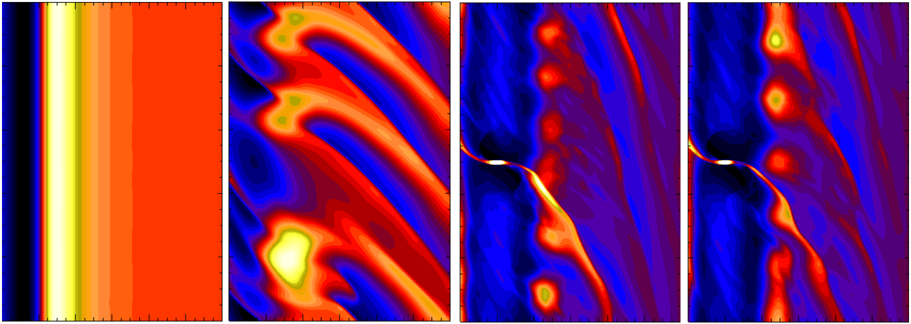

3D disk with viscosity jump in radius 3D self-gravitating disk-planet simulation

[Note: global simulations plotted in a box ($r \to x$, $\phi \to y$)]

Dust-trapping

Meheut et al. (2012): add dust to RWI-unstable disk

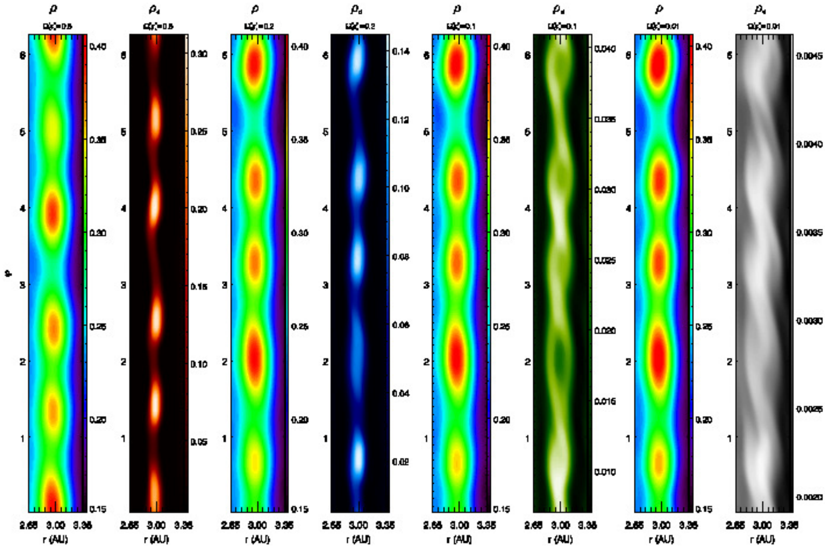

Dust-trapping

Particle concentration v.s. turbulent diffusion (Lyra & Lin, 2013)

$$\frac{\partial \rho_d}{\partial t} + \nabla \cdot (\rho_d \mathbf{v}_d) = D\nabla^2 \rho_d$$

- D: from instability of vortex core$\rightarrow$ e.g. elliptic instability (Lesur & Papaloizou, 2010)

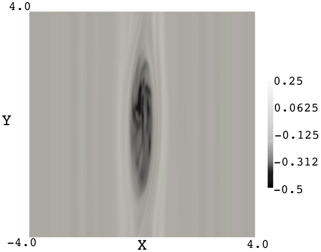

- $\mathbf{v}_d = \mathbf{v}_g + \tau c_s^2 \nabla \ln \rho_g$, isothermal gas
- $\mathbf{v}_g$ from model of an elliptic vortex (e.g. Kida vortex)
- τ friction time

Dust-trapping

Steady-state dust distribution in elliptic vortices (Lyra & Lin, 2013)

$$\rho_d(a) \propto \exp\left(-k^2a^2/4\right)$$

(EXACT solution possible!)

- $a \sim$ distance from vortex centre
- k depends on vortex aspect-ratio χ, friction time τ and diffusion D

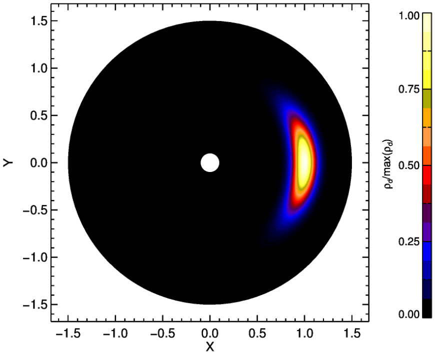

Dust-trapping

Steady-state dust distribution in elliptic vortices (Lyra & Lin, 2013)

$$\rho_d(a) \propto \exp\left(-k^2 a^2/4\right)$$

(EXACT solution possible!)

- $a \sim$ distance from vortex centre
- k depends on vortex aspect-ratio χ, friction time τ and diffusion D

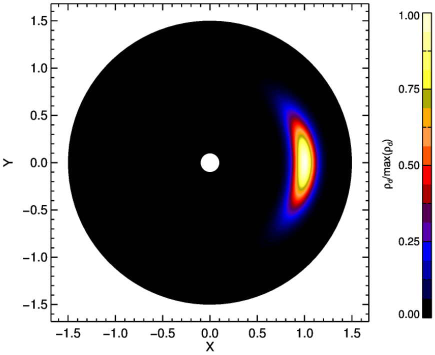

Dust-trapping

Steady-state dust distribution in elliptic vortices (Lyra & Lin, 2013)

$$\rho_d(a) \propto \exp\left(-k^2a^2/4\right)$$

(EXACT solution possible!)

- $a \sim$ distance from vortex centre
- k depends on vortex aspect-ratio χ, friction time τ and diffusion D

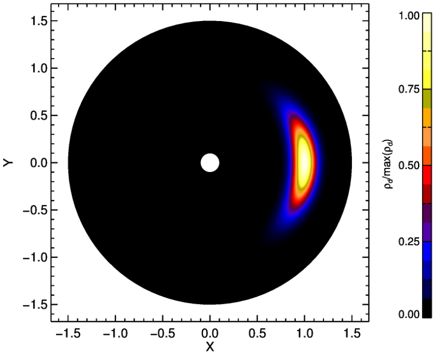

Square one: the linear instability

The original linear problem (Lovelace et al., 1999):

adiabatic non-self-gravitating 2D disk with radial structure

Recent generalizations:

- Self-gravity 2D (Lin & Papaloizou, 2011a,b; Lovelace & Hohlfeld, 2013)
- Magnetic fields 2D (Yu & Li, 2009; Yu & Lai, 2013)
- Isothermal 3D (Meheut et al., 2012)

My efforts:

- Polytropic 3D (Lin, 2012a, 2013a)
- Adiabatic 3D (Lin, 2013b)

Linear problem for 3D polytropic disks ($p \propto \rho^{1+1/n}$)

1. Steady, axisymmetric, vertically hydrostatic density bump at $r = r_0$
2. Perturb fluid equations, e.g. $\rho \to \rho + \delta\rho(r,z)\exp i(m\phi + \sigma t)$
3. Combine linear equations to get equation for $W \equiv \delta p/\rho$:

$$L(r,z;\sigma)W = 0.$$

- $W \to$ eigenfunction ; $\sigma \to$ eigenvalue

Very complicated PDE even for numerical work!

Linear problem for 3D polytropic disks ($p \propto \rho^{1+1/n}$)

1. Steady, axisymmetric, vertically hydrostatic density bump at $r = r_0$
2. Perturb fluid equations, e.g. $\rho \to \rho + \delta\rho(r, z) \exp i(m\phi + \sigma t)$
3. Combine linear equations to get equation for $W \equiv \delta p/\rho$:

$$L(r, z; \sigma)W = 0.$$

- $W \to$ eigenfunction ; $\sigma \to$ eigenvalue

Very complicated PDE even for numerical work!
Reduction to 1D

$$W(r, z) = \sum_{l=0}^{\infty} W_l(r)\mathcal{C}_l^{\lambda}(z/H),$$

where $\mathcal{C}_l^{\lambda}(x)$ are Gegenbauer polynomials.

$$L(r, z; \sigma)W = 0 \to A_l(W_l) + B_l(W_{l-2}) + C_l(W_{l+2}) = 0.$$

Example problem

$n = 1.5$ polytrope with a surface density bump

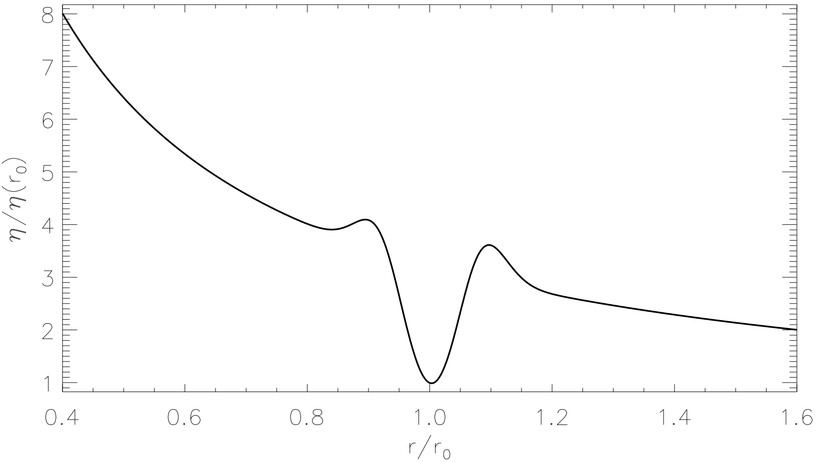

Recall $\eta = \frac{1}{r\Sigma}\frac{d}{dr}\left(r^2\Omega\right)$ is the potential vorticity (note: RWI for PV minima only)

Example solution

$$W(r,z) = W_0(r) + W_2(r)\mathcal{C}_2^{\lambda}(z/H) + \cdots$$

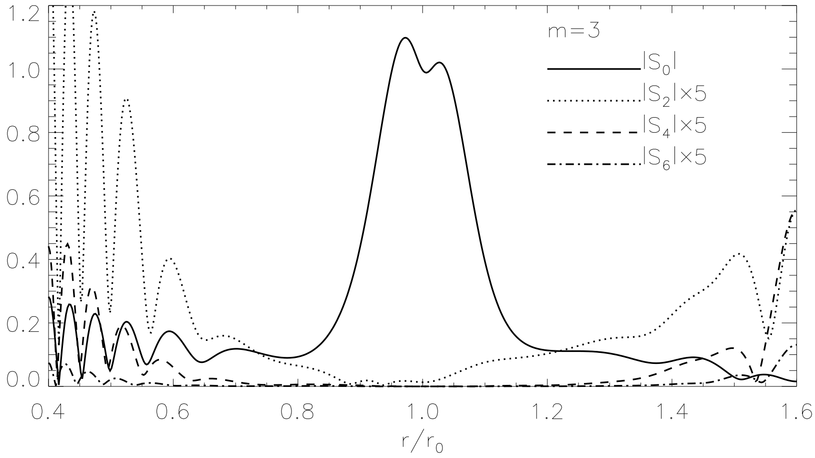

Growth rate $\sim 0.1\Omega$, same as 2D ($l_{\max} \equiv 0$). Instability is 2D.

Horizontal flow

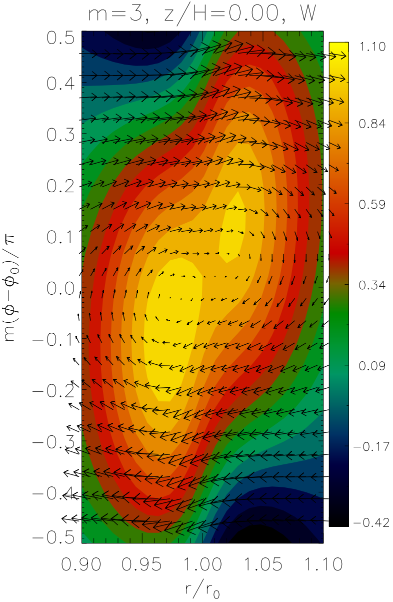

Anti-cyclonic motion associated with over-density

Vertical flow at vortex centre

Magnitude of vertical motion decreases with increasing n (more compressible)

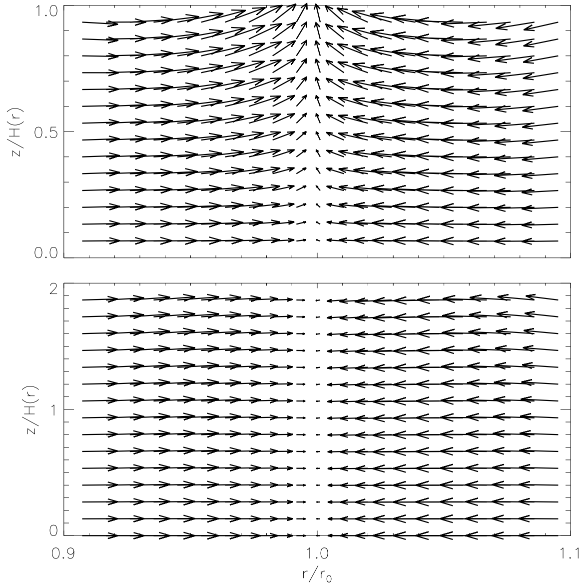

$\leftarrow$ $n = 1.0$ polytrope

$\leftarrow$ vertically isothermal disk ($n = \infty$, special treatment with Hermite polynomials)

Comparison to non-linear simulations

Upward motion seen in non-linear hydrodynamic simulations of Meheut et al. (2012):

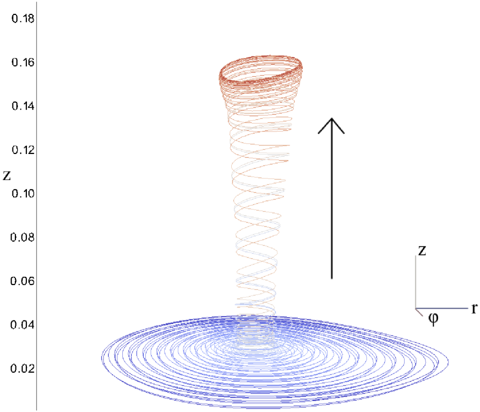

Meheut et al. (2012) $\rightarrow$ mm dust lifted to disk surface

Extension to adiabatic 3D disks

- $p \propto \rho^{\Gamma}$ in basic state only
- Energy equation $Ds/Dt = 0$, $s \equiv p/\rho^{\gamma} \propto \rho^{\Gamma-\gamma}$
- $\gamma \geq \Gamma \geq 1$, density bump $\rightarrow$ entropy dip

$$V_1 W + \overline{V}_1 Q = 0$$
$$V_2 W + \overline{V}_2 Q = 0$$

- $W = \delta p/\rho \rightarrow$ pressure perturbation
- $Q = c_s^2 \delta\rho/\rho \rightarrow$ density perturbation
- $S \equiv W - Q \rightarrow$ entropy perturbation

Finite-difference/pseudo-spectral method:

$$W(r_i, z) \equiv W_i(Z) = \sum_{k=1}^{N_z} w_{ki}\psi_k(Z/Z_{\mathrm{max}})$$

[$\psi_k = T_{2(k-1)}$ are Chebyshev polynomials]

Non-homentropic example

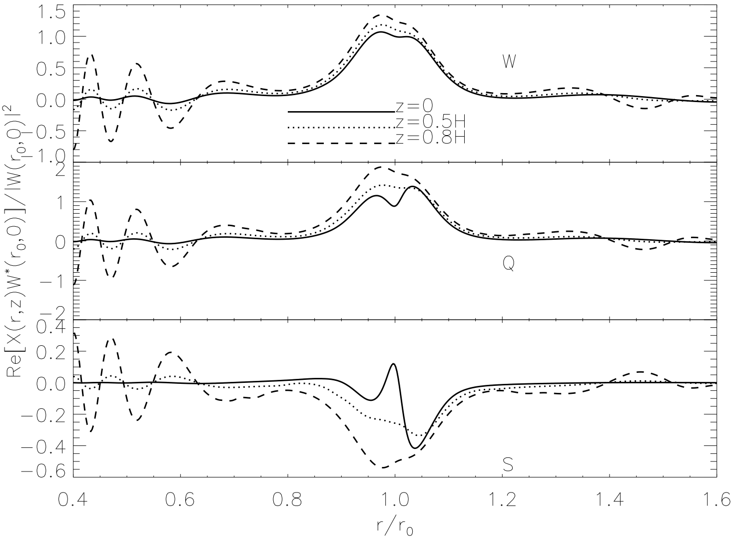

$\Gamma = 1.67$, $\gamma = 2.5$, $m = 3$ along $\phi = \phi_0$.
Growth rate $0.1099\Omega_0$ (cf. $0.1074\Omega_0$ for $\gamma = 1.67$)

Baroclinity, $\nabla P \times \nabla \rho \neq 0$

$$\overline{S} \equiv Q - \frac{\gamma}{\Gamma} W$$

$\rightarrow$ a measure of baroclinity ($= 0$ if $\Gamma = \gamma$)

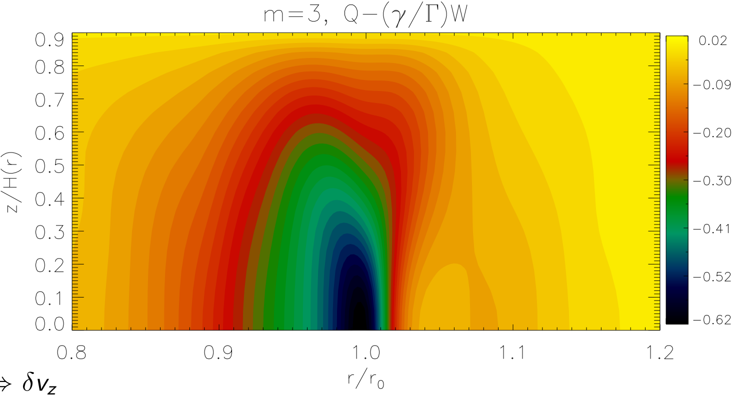

- $\bar{S} \Rightarrow \delta v_z$
- $\nabla \bar{S} \Rightarrow (\nabla \times \boldsymbol{\delta}\mathbf{v})_\phi$

Meridional vortical motion

$\Gamma = 1.67$, $\gamma = 2.5$, $m = 5$ along $\phi = \phi_0$

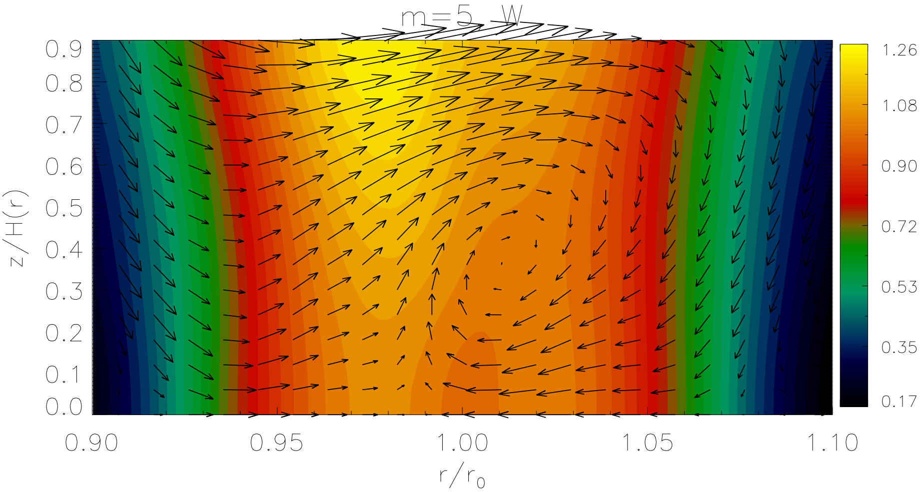

Vertical motion

Kato (2001):

$$\delta v_z \sim -\frac{\nu}{N_z^2}\frac{\partial W}{\partial z} - \nu\rho\left(\frac{\partial p}{\partial z}\right)^{-1} W, \quad N_z^2 \neq 0$$

at co-rotation radius, and ν here is the growth rate.

$$\left[\text{c.f.} \qquad \delta v_z \sim -\frac{1}{\nu}\frac{\partial W}{\partial z}, \quad N_z^2 \equiv 0.\right]$$

Notice for $N_z^2 \neq 0$

$$\frac{\text{pressure}}{\text{buoyancy}} \sim \frac{\Omega^2}{N_z^2}\frac{\partial \ln W}{\partial \ln z},$$

i.e. buoyancy dominates at large z as N_z^2 increases with height.

Origin of δv_z is different between homentropic and non-homentropic flow

Comparison with hydrodynamic simulations

- Isothermal disk, adiabatic evolution ($\Gamma \equiv 1$, $\gamma = 1.4$)

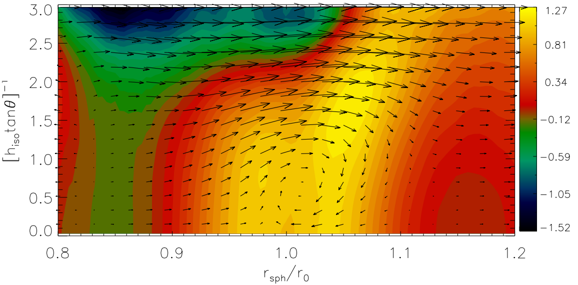

← ZEUS simulation

$$\mathrm{Re}(\sigma) = -0.99 m\Omega_0$$
$$\mathrm{Im}(\sigma) = -0.194\Omega_0$$

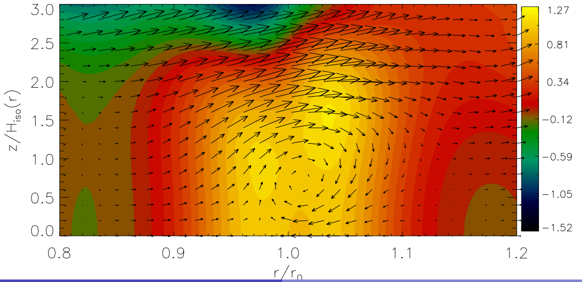

← linear code

$$\mathrm{Re}(\sigma) = -0.9896 m\Omega_0$$
$$\mathrm{Im}(\sigma) = -0.1937\Omega_0$$

Comparison with hydrodynamic simulations

- Isothermal disk, adiabatic evolution ($\Gamma \equiv 1$, $\gamma = 1.4$)

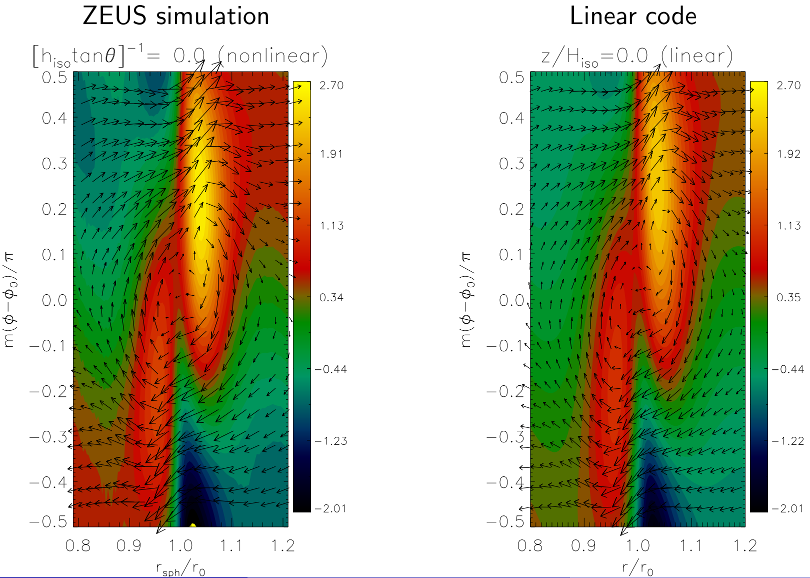

Vortex-formation in layered-accretion disks?

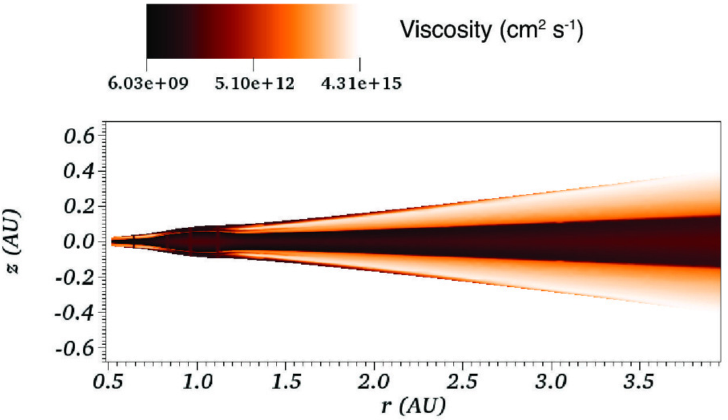

(Axisymmetric model from Landry et al., 2013)

- RWI requires low viscosity, but only have dead zone near midplane
- Rossby vortices have weak vertical structure (vorticity columns)

Linear RWI in layered disks

First task for any linear problem: equilibrium state. But:

- Need localized radial gradient for RWI
- Want a viscous atmosphere

Linear RWI in layered disks

First task for any linear problem: equilibrium state. But:

- Need localized radial gradient for RWI
- Want a viscous atmosphere

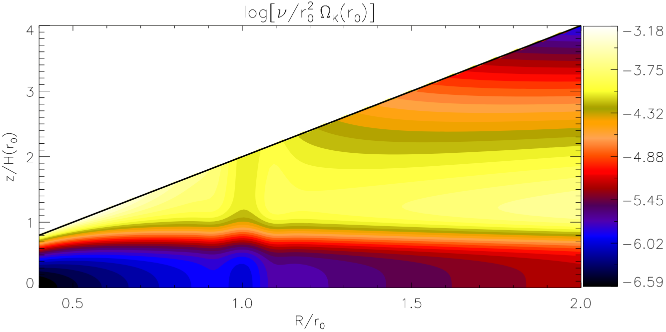

(Lin, 2014)

- Choose viscosity and v_R s.t. $R\rho v_R = \dot{M}(z)$
- Strictly isothermal gas

PLUTO simulations of layered disks

Spherical grid, $z \in [0, 2H]$ at $R = r_0$.
ν decreases by 10^2 from active (upper) to dead (lower) layer.

- Case 1: all dead, linear growth rate $= 0.199\Omega$
  ($\alpha \sim 10^{-4}$)
- Case 2: half dead, linear growth rate $= 0.182\Omega$
  ($\alpha \sim 10^{-4}$ for $z \in [0, H]$; $\alpha \sim 10^{-2}$ for $z \in [H, 2H]$)

Local viscous time $H^2/\nu \gg t_{\mathrm{RWI}}$

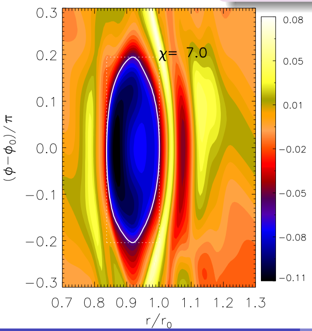

←Rossby numbers→
← Case 1
Case 2 →

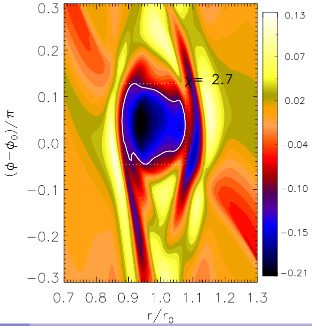

Disk-planet interaction in layered disks

Standard result for Jupiter-mass planet in a low viscosity unlayered disk ($\alpha \sim 10^{-4}$)

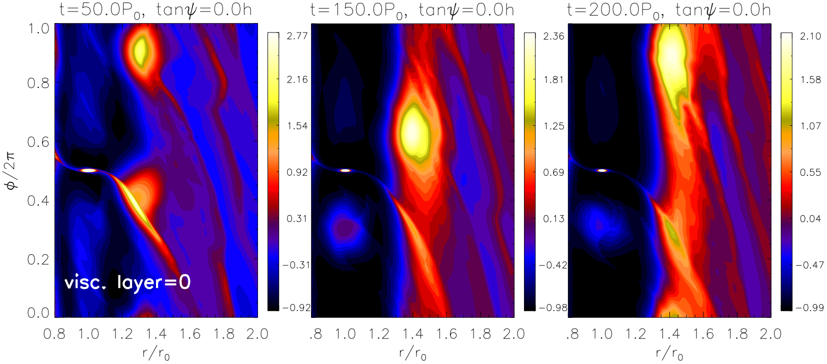

Disk-planet interaction in layered disks

Repeat simulation with layered viscosity

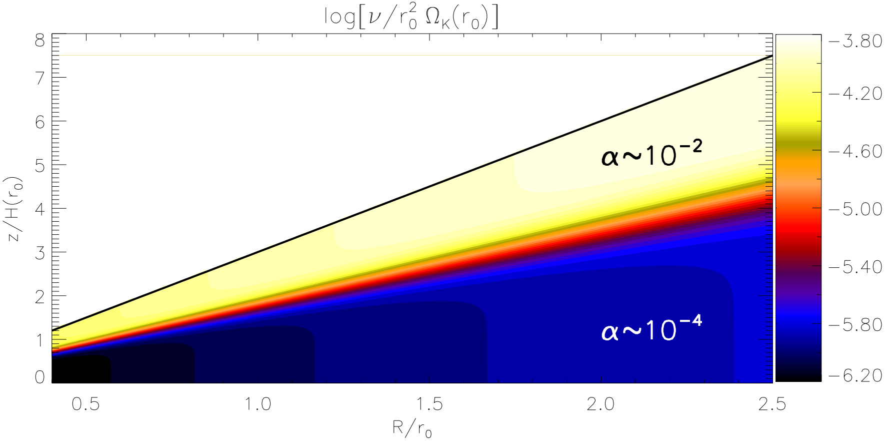

Disk-planet interaction in layered disks

Rossby vortex does not survive against viscous layer

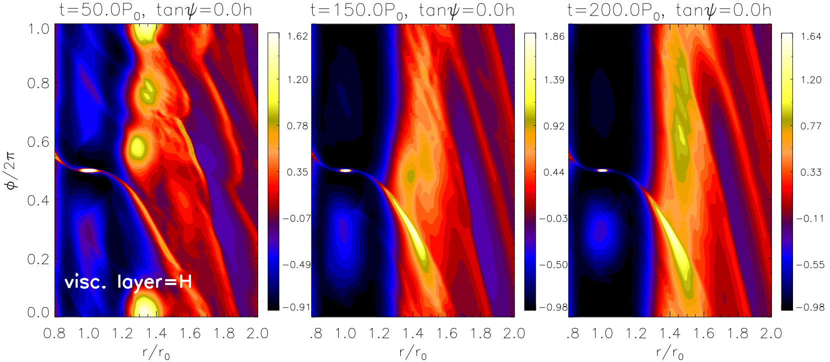

Vertical domain size: $z \in [0, 3H]$, viscous layer $z \in [2, 3H]$, $\Sigma_{\mathrm{visc}}/\Sigma \sim 0.04$

- Lesson: long term vortex formation sensitive to disk vertical structure
- Next step: back-reaction on α

Disk-planet interaction in layered disks

Restart a low-viscosity simulation with a viscous atmosphere

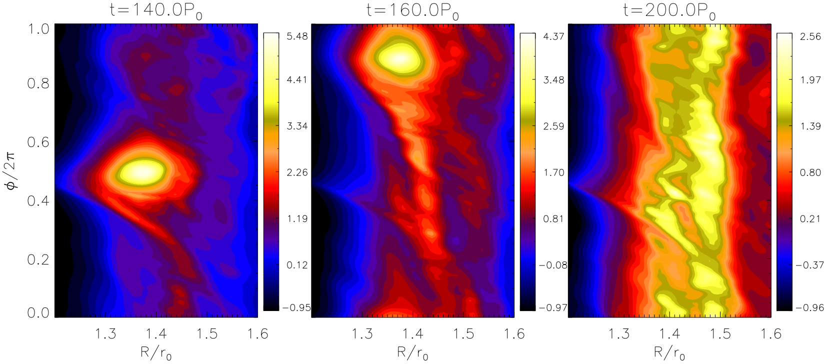

Vertical domain size: $z \in [0, 3H]$, viscous layer $z \in [2, 3H]$, $\Sigma_{\rm visc}/\Sigma \sim 0.04$

- Lesson: long term vortex formation sensitive to disk vertical structure
- Next step: back-reaction on α

Self-gravitating disks

- Observe large-scale structures at 10s of AU
- Wide-orbit giant planets

Self-gravitating disks

- Observe large-scale structures at 10s of AU
- Wide-orbit giant planets

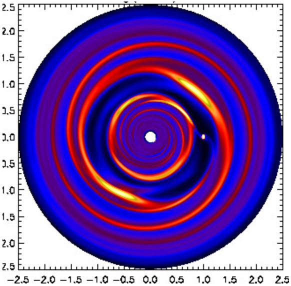

$M_{\rm disk} = 0.08 M_*$

$Q_{\rm out} = 1.5$

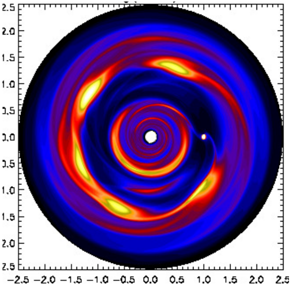

$M_{\rm disk} = 0.056 M_*$

$Q_{\rm out} = 3$

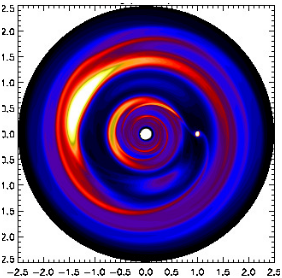

$M_{\rm disk} = 0.021 M_*$

$Q_{\rm out} = 8$

(ZEUS simulations in 3D, Lin, 2012b)

Stabilization of the vortex mode by self-gravity

The 2D linear problem with self-gravity:

$$L(S) = \delta\Sigma, \quad S = c_s^2 \delta\Sigma/\Sigma + \delta\Phi, \quad \delta\Phi = \int K(r, r')\delta\Sigma(r')dr'$$

Stabilization of the vortex mode by self-gravity

The 2D linear problem with self-gravity:

$$L(S) = \delta\Sigma, \quad S = c_s^2\delta\Sigma/\Sigma + \delta\Phi, \quad \delta\Phi = \int K(r, r')\delta\Sigma(r')dr'$$

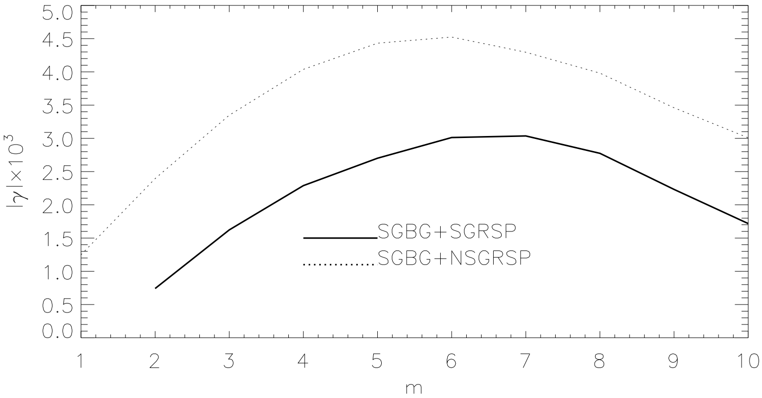

($|\gamma|$ here is growth rate). Solid: with self-gravity. Dotted: no self-gravity.
[See Lin & Papaloizou (2011a) for formal proof]

Vertical self-gravity

Self-gravity in 3D $[\min(Q_T) = 8]$:

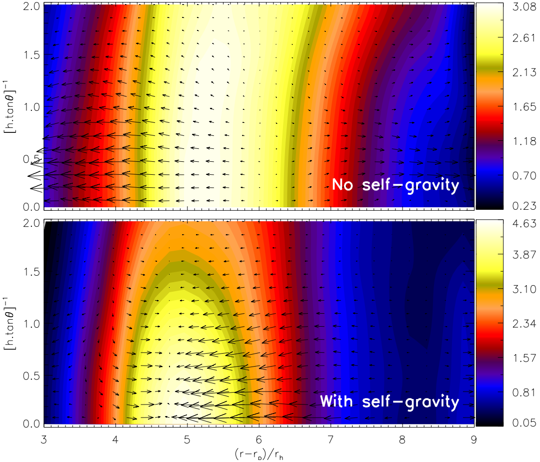

(Global 3D ZEUS simulations, Lin, 2012b).

Lesson: non-SG initial disk may not remain so

Gravitational edge instabilities

GI associated with gaps or edges even when Toomre stability criterion satisfied ($Q_T > 1$ everywhere)

- Lovelace & Hohlfeld (1978); Sellwood & Kahn (1991): galactic/stellar disks
- Meschiari & Laughlin (2008): gaps in gaseous protoplanetary disks
- Lin & Papaloizou (2011b): confirmation of GEI for planet gaps (PV max.)

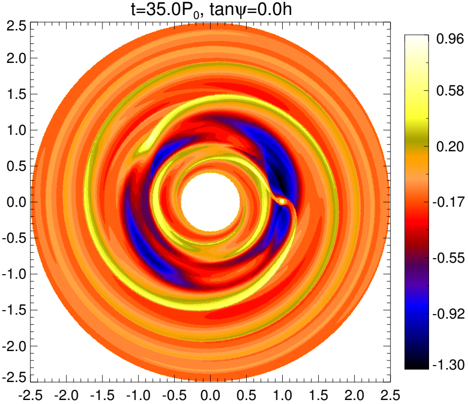

PLUTO simulation

Gravitational edge instabilities

GI associated with gaps or edges even when Toomre stability criterion satisfied ($Q_T > 1$ everywhere)

- Lovelace & Hohlfeld (1978); Sellwood & Kahn (1991): galactic/stellar disks
- Meschiari & Laughlin (2008): gaps in gaseous protoplanetary disks
- Lin & Papaloizou (2011b): confirmation of GEI for planet gaps (PV max.)

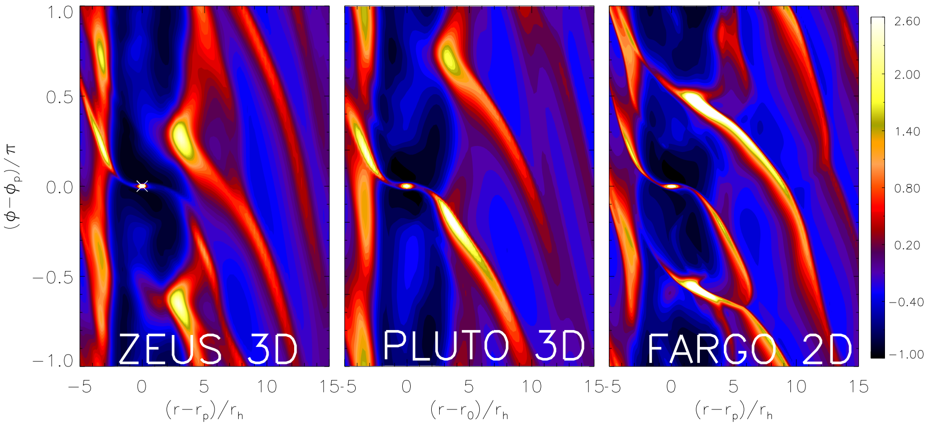

Influence of GEI on disk-planet torques

Spirals supply material to execute horseshoe turns ahead of planet

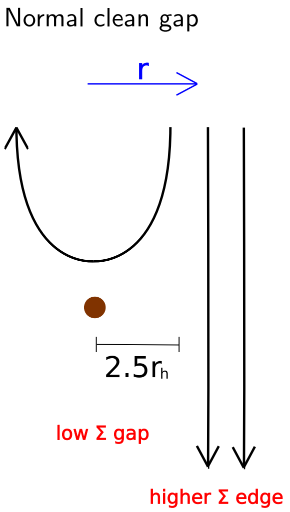

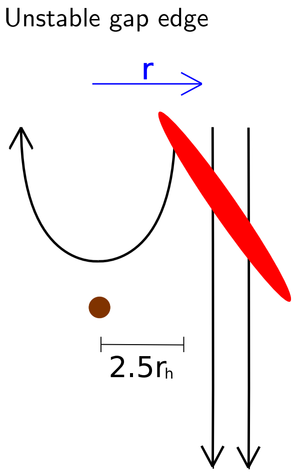

→ positive co-orbital torques

Outward migration induced by an unstable gap

FARGO simulations

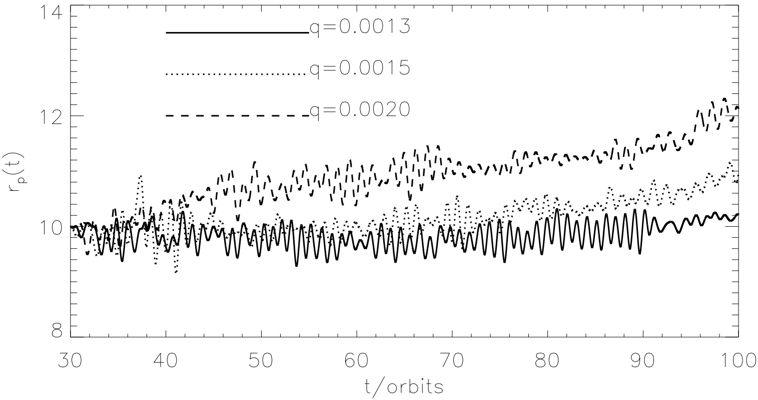

(CITA summer student project, Cloutier & Lin, 2013)

- $q \equiv M_p/M_*$
- Larger $M_p \rightarrow$ deeper gap (lower surface density) but stronger GI because of sharper gap edge$\rightarrow$ larger torques

Type III migration triggered by the unstable gap

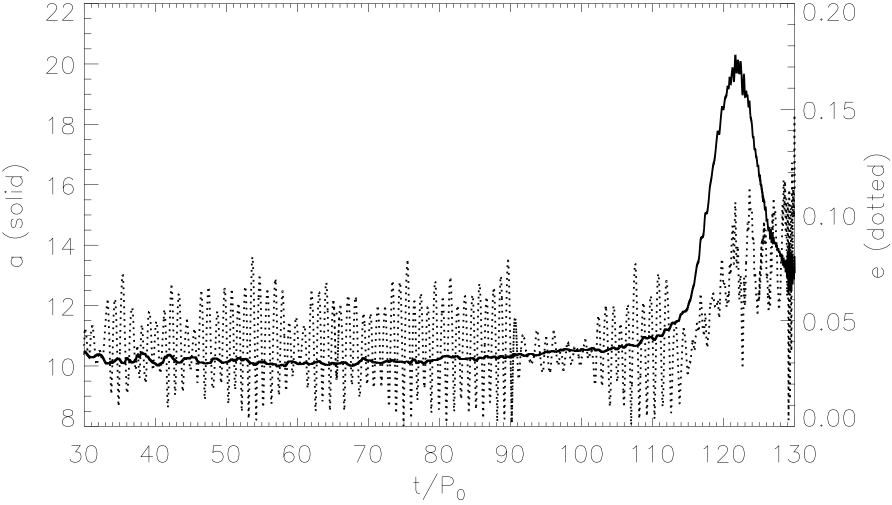

(Cloutier & Lin, 2013)

Type III migration triggered by the unstable gap

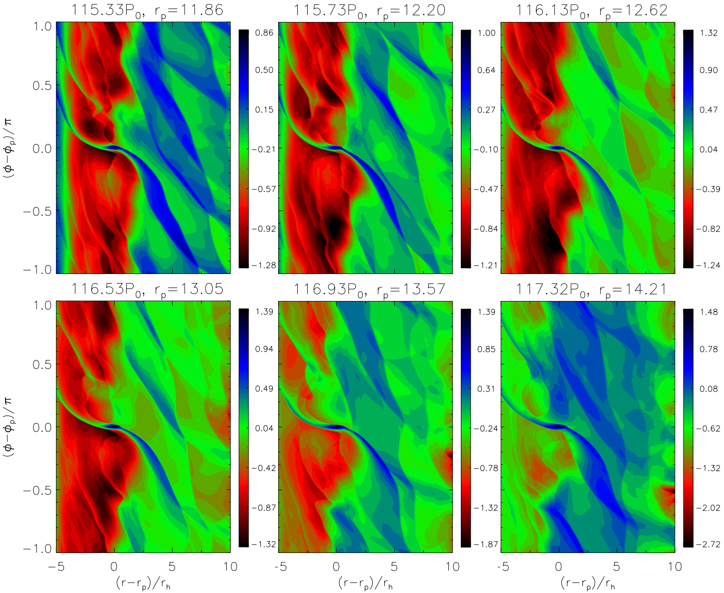

Long-period giant planets/brown dwarfs

Star	M_p/M_J	r_p/AU
Oph 11	21 ± 3	243 ± 55
CHXR 73	15^{+8}_{-5}	210
DH Tau	11^{+3}_{-10}	330
CD-35 2722	31 ± 8	67
GSC 06214-00210	17 ± 3	320
Ross 458(AB)	8.5 ± 2.5	1170
GQ Lup	21.5 ± 20.5	103
1RXS J1609	≈ 8	330
CT Cha	17	440
AB Pic	13.5 ± 0.5	260
HN Peg	16 ± 9	795 ± 15
HR 8799	5–10	15–68
Fomalhaut	$3^{+1.2}_{-0.5}$	119

(Adapted from Vorobyov, 2013)

Implications for models of wide-orbit giant planet formation by disk fragmentation

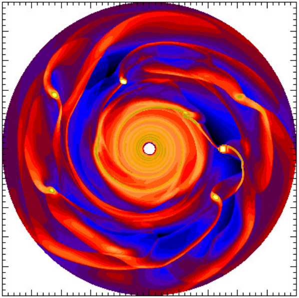

- Zhu et al. (2012); Vorobyov (2013): most clumps fall in, but occasionally can survive by opening gaps
- Our simulations $\rightarrow$ gap stability may be another issue
- Zhu et al.: additional clump formation along edge of a gap opened by a previous clump; Vorobyov: clump migrates outward

MHD plus gravity from scratch

Standard shearing box resistive MHD, plus Poisson

$$\begin{aligned}
&\frac{\partial\rho}{\partial t} + \nabla\cdot(\rho\mathbf{v}) = 0,\\
&\frac{\partial\mathbf{v}}{\partial t} + \mathbf{v}\cdot\nabla\mathbf{v} + 2\Omega_0\hat{\mathbf{z}}\times\mathbf{v} = -\frac{1}{\rho}\nabla\Pi + \frac{1}{\rho\mu_0}\mathbf{B}\cdot\nabla\mathbf{B} - \nabla\Phi,\\
&\frac{\partial\mathbf{B}}{\partial t} = \nabla\times\left(\mathbf{v}\times\mathbf{B} - \eta\nabla\times\mathbf{B}\right),\\
&\nabla^2\Phi_d = 4\pi G\rho,
\end{aligned}$$

$\Phi = \Phi_{\mathrm{ext}} + \Phi_d$, $\Pi = P(\rho) + |\mathbf{B}|^2/2\mu_0$

MHD plus gravity from scratch

Linearize $\rightarrow$

$$\frac{\mathrm{i}\sigma}{c_s^2}W + \mathrm{i}k_x\delta v_x + (\ln\rho)'\,\delta v_z + \delta v_z' = 0,$$

$$\mathrm{i}\sigma\delta v_x - 2\Omega\delta v_y = -\mathrm{i}k_x\tilde{W} + \frac{B_z}{\mu_0\rho}\left[\delta B_x' - \mathrm{i}k_x\left(\delta B_z + \epsilon\delta B_y\right)\right],$$

$$\mathrm{i}\sigma\delta v_y + \frac{\kappa^2}{2\Omega}\delta v_x = \frac{B_z}{\mu_0\rho}\delta B_y',$$

$$\mathrm{i}\sigma\delta v_z = -\tilde{W}' - \frac{B_y}{\mu_0\rho}\delta B_y',$$

$$\mathrm{i}\bar{\sigma}\delta B_x = B_z\delta v_x' + \eta\delta B_x'' + \eta'\delta B_x' - \mathrm{i}k_x\eta'\delta B_z,$$

$$\mathrm{i}\bar{\sigma}\delta B_y = B_z\delta v_y' - B_y\Delta - S\delta B_x + \eta\delta B_y'' + \eta'\delta B_y',$$

$$\mathrm{i}\bar{\sigma}\delta B_z = -\mathrm{i}k_xB_z\delta v_x + \eta\delta B_z'',$$

$$\delta\Phi'' - k_x^2\delta\Phi = \frac{\rho}{c_s^2 Q}W.$$

$'\equiv d/dz$, $\mathrm{i}\bar{\sigma} = \mathrm{i}\sigma + k_x^2\eta$, $\tilde{W} = W + \delta\Phi$, $W = c_s^2\delta\rho/\rho$, $\Delta \equiv \nabla\cdot\delta\mathbf{v}$, $\epsilon = B_y/B_x$, $Q = \Omega^2/4\pi G\rho(0)$

MHD plus gravity from scratch

Reduction to hydrodynamics

$$L \begin{bmatrix} \delta v_x \\ \delta v_y \\ W \\ \delta \Phi \end{bmatrix} = 0.$$

MHD plus gravity from scratch

Reduction to hydrodynamics

$$L \begin{bmatrix} \delta v_x \\ \delta v_y \\ W \\ \delta\Phi \end{bmatrix} = 0.$$

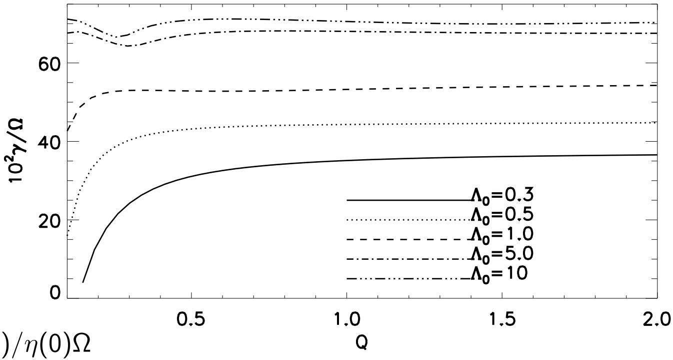

$\Lambda_0 = v_A^2(0)/\eta(0)\Omega$

MHD plus gravity from scratch

Reduction to hydrodynamics

$$L \begin{bmatrix} \delta v_x \\ \delta v_y \\ W \\ \delta\Phi \end{bmatrix} = 0.$$

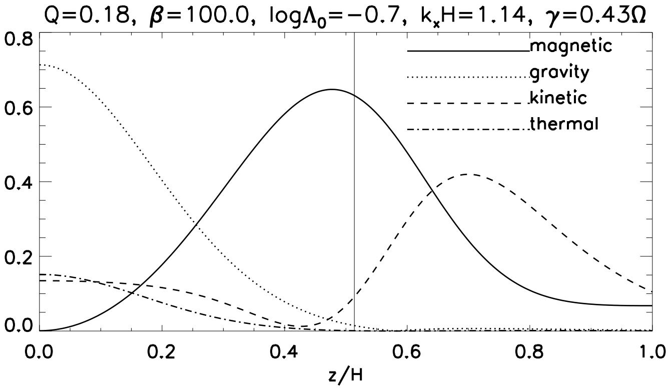

Future

Linear

- Global self-gravitating disk models in 3D, vertical self-gravity
- Thermodynamics
- Baroclinic disks ($\partial_z\Omega \neq 0$)

Non-linear

- Self-gravitating vortices in 3D
- Gravitational instability of disk edges

Future

Linear

- Global self-gravitating disk models in 3D, vertical self-gravity
- Thermodynamics
- Baroclinic disks ($\partial_z \Omega \neq 0$)

Non-linear

- Self-gravitating vortices in 3D
- Gravitational instability of disk edges

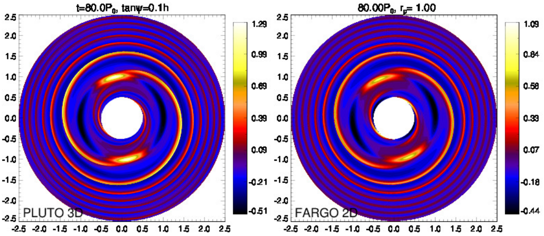

Future

Linear

- Global self-gravitating disk models in 3D, vertical self-gravity
- Thermodynamics
- Baroclinic disks ($\partial_z \Omega \neq 0$)

Non-linear

- Self-gravitating vortices in 3D
- Gravitational instability of disk edges
- Long-term goal: global resistive MHD plus gravity (layered disks, episodic accretion)
- Gap stability in non-isothermal disks (2014 CITA summer student project)
- Outward migration of giant planets

Future

Linear

- Global self-gravitating disk models in 3D, vertical self-gravity
- Thermodynamics
- Baroclinic disks ($\partial_z \Omega \neq 0$)

Non-linear

- Self-gravitating vortices in 3D
- Gravitational instability of disk edges
- Long-term goal: global resistive MHD plus gravity (layered disks, episodic accretion)
- Gap stability in non-isothermal disks (2014 CITA summer student project)
- Outward migration of giant planets

References

Armitage P. J., 2011, ARAA, 49, 195

Avenhaus H., Quanz S. P., Schmid H. M., Meyer M. R., Garufi A., Wolf S., Dominik C., 2014, ApJ, 781, 87

Barge P., Sommeria J., 1995, A&A, 295, L1

Cloutier R., Lin M.-K., 2013, MNRAS, 434, 621

Debes J. H., Jang-Condell H., Weinberger A. J., Roberge A., Schneider G., 2013, ApJ, 771, 45

Goodman J., Narayan R., Goldreich P., 1987, MNRAS, 225, 695

Grady C. A., Muto T., Hashimoto J., Fukagawa M., Currie T., Biller B., Thalmann C., Sitko M. L., 2013, ApJ, 762, 48

Isella A., Pérez L. M., Carpenter J. M., Ricci L., Andrews S., Rosenfeld K., 2013, ApJ, 775, 30

Kato S., 2001, PASJ, 53, 1

Kida S., 1981, Journal of the Physical Society of Japan, 50, 3517

Landry R., Dodson-Robinson S. E., Turner N. J., Abram G., 2013, ApJ, 771, 80

Lesur G., Papaloizou J. C. B., 2010, A&A, 513, A60

Li H., Colgate S. A., Wendroff B., Liska R., 2001, ApJ, 551, 874

Lin M.-K., 2012a, ApJ, 754, 21

Lin M.-K., 2012b, MNRAS, 426, 3211

Lin M.-K., 2013a, MNRAS, 428, 190

Lin M.-K., 2013b, ApJ, 765, 84

Lin M.-K., 2014, MNRAS, 437, 575

Lin M.-K., Papaloizou J. C. B., 2010, MNRAS, 405, 1473

Lin M.-K., Papaloizou J. C. B., 2011a, MNRAS, 415, 1426

Lin M.-K., Papaloizou J. C. B., 2011b, MNRAS, 415, 1445

Lovelace R. V. E., Hohlfeld R. G., 1978, ApJ, 221, 51

Lovelace R. V. E., Hohlfeld R. G., 2013, MNRAS, 429, 529

Lovelace R. V. E., Li H., Colgate S. A., Nelson A. F., 1999, ApJ, 513, 805

Lyra W., Lin M.-K., 2013, ApJ, 775, 17

Lyra W., Mac Low M.-M., 2012, ApJ, 756, 62

Meheut H., Keppens R., Casse F., Benz W., 2012, A&A, 542, A9

Meheut H., Lovelace R. V. E., Lai D., 2013, MNRAS, 430, 1988

Meheut H., Meliani Z., Varniere P., Benz W., 2012, A&A, 545, A134

Meheut H., Yu C., Lai D., 2012, MNRAS, 422, 2399

Meschiari S., Laughlin G., 2008, ApJL, 679, L135

Papaloizou J. C. B., Pringle J. E., 1985, MNRAS, 213, 799

Quanz S. P., Avenhaus H., Buenzli E., Garufi A., Schmid H. M., Wolf S., 2013, ApJL, 766, L2

Sellwood J. A., Kahn F. D., 1991, MNRAS, 250, 278

van der Marel N., van Dishoeck E. F., Bruderer S., Birnstiel T., Pinilla P., Dullemond C. P., van Kempen T. A., Schmalzl M., Brown J. M., Herczeg G. J., Matthews G. S., Geers V., 2013, Science, 340, 1199

Vorobyov E. I., 2013, A&A, 552, A129

Yu C., Lai D., 2013, MNRAS, 429, 2748

Yu C., Li H., 2009, ApJ, 702, 75

Zhu Z., Hartmann L., Nelson R. P., Gammie C. F., 2012, ApJ, 746, 110